Geophysical Research Letters

Supporting Information for

Decoding the interplay between tidal notch geometry and sea-level variability during the Last Interglacial (Marine Isotopic Stage 5e) high stand

Nikos Georgiou[1,2*], Paolo Stocchi[3], Elisa Casella[1], Alessio Rovere[1]

[1] Ca' Foscari University of Venice, Department of Environmental Sciences, Informatics and Statistics, Scientific Campus, via Torino 155, 30172 Mestre (VE), Italy.

[2] University of Patras, Department of Geology, Panepistimioupoli, 265 04 Rio, Patra, Greece.

[3] NIOZ- Royal Netherlands Institute for Sea Research, Landsdiep 4, 1797 SZ 't Horntje, Texel, Netherlands.

Contents of this file

Introduction

Below are described in detail: the methodology followed for the development of the 3d Digital Elevation Model of the Orosei Cliff in Text S1, the geomorphological analysis and methodology followed to exclude the not well-preserved parts of the cliff in Text S2 and Figure S1, and the Table S1 which contains the final fitting scores of the modeled notches to the original Measured Notch Profiles.

Text S1. Details on Photogrammetry

SfM-MVS merges photogrammetric principles with advances in 3D computer vision algorithms (Carrivick et al., 2016). The approach requires as an input a dataset of overlapping photographs of the study area. The photoshoot was operated onboard while keeping the vessel at an almost constant distance from the cliff. Stainless rulers were manually placed on the notch and were used to scale the reconstructed 3D model of the notch, optimize the image alignment, and minimize the sum of the reprojection error of the estimated internal camera parameters and point cloud in the SfM-MVS method. A Canon EOS 77D camera with 55mm focal length, resolution of 6000x4000 pixels, and pixel size of 3.84 x 3.84 μm was used for the process. Metashape generates 3D models and orthorectified images from overlapping photos through the SfM-MVS approach. The first step of this process is accomplished through pho-to alignment using the SfM algorithm (Ullman, 1979). The algorithm produces a 3D point cloud of the surveyed area, the relative position of the photographs collected, and the internal calibration parameters (focal

length, principal point location and radial, and tangential distortion coefficients) (Casella et al., 2016). 121 photos were used to build the orthomosaic and the 3D model. Photos were collected at a distance from the cliff of about 60m. The resolution of the orthomosaic is 3.97mm/pix. The reprojection error is 1.02 pix, while the control scale bars error was estimated to 0.0046m. The area of the cliff that was mapped is 3070 m^2.

Text S2. Notch geomorphometric analysis

- The slope was employed to identify cliff sections with a steep incline. These sections were often associated with deterioration from mechanical erosion or calcite accumulation, deviating from the smooth curvature typically observed in the fossil notch morphology (Fig. S1a).

- Aspect (orientation) refers to the direction that the surface slope faces. Aspect proved a useful tool that aids in keeping track of the flowstone-like calcite accretion (Fig. S1b - brown color), which is mainly flowing from the overhanging cliff while changing its orientation. In addition, it supplies information regarding the cliff collapse since the morphology and orientation of the notch are altered in the areas where this phenomenon is observed.

- Ruggedness describes a measure of surface roughness and local heterogeneity titled Vector Ruggedness Measure (VRM) (Fig. S1c). Due to the smoothness of the notch indentation, this attribute helps in distinguishing the rough surfaces created by calcite accretion. The combination of this attribute with aspect constitutes a reliable tool for the recognition of the calcite accretion features.

- Color variation (discoloration) along the notch surface was co-estimated for the selection of the unaffected notch segments. Greyish colors, which were mostly detected close to the floor of the fossil notch (Fig. S1d, e), display areas where the notch's floor is missing since it was affected possibly by cliff collapse triggered by rock boulder fall, mainly originating from the overhanging cliffs. The black discoloration of the limestone cliffs is usually correlated to organic material deterioration and is accompanied by light-greyish calcite accretion. Due to the color variation of the calcite accretion with the original notch, the attributes of aspect and ruggedness were mostly followed for the recognition of these features.

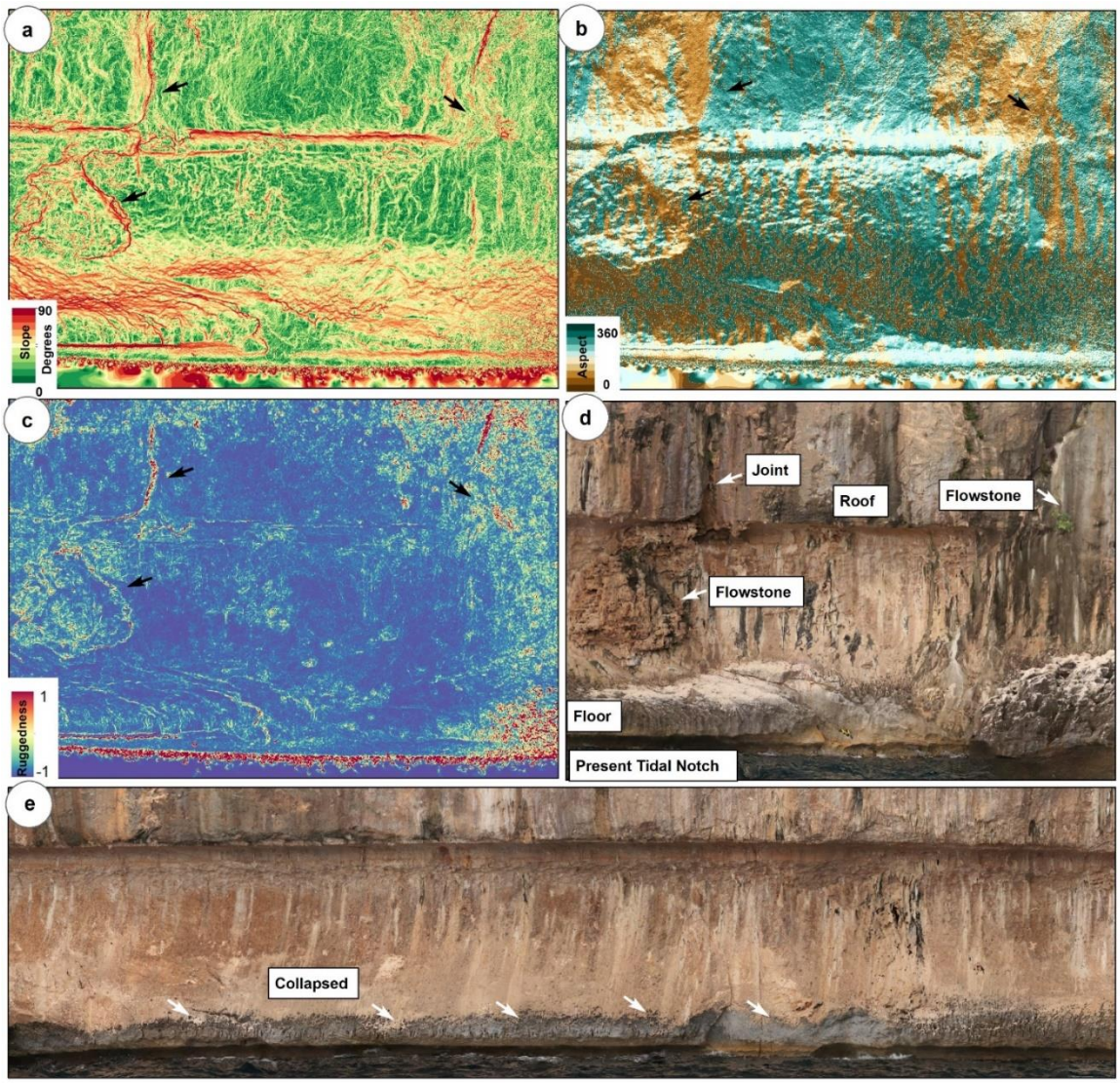

Figure S1. Typical example of an excluded segment of the notch: a. Slope Gradient, b. Aspect, c. Ruggedness, d. Orthomosaic showing the roof, floor of the notch and the effects of the local factors, e. Part of the orthomosaic showing the missing floor of the notch locally due to mechanical erosion.

Table S1. Best and average fitting results of the clusters derived through the methodological approach described in section 2.3 of the main text. The results are categorized based on the variable of erosion rate (0.25-2 mm/a) increasing horizontally rightwards and on their complexity (single rise, 1 to 3+ peaks) increasing vertically. The best fitting cluster is also signed above the fitting score.

	Erosion rate (mm/a)	0.25		0.5		0.75		1		2	
	Linear Regression	Pos	Neg	Pos	Neg	Pos	Neg	Pos	Neg	Pos	Neg
Single rise	AVG fit			Cluster 1	Cluster 1	Cluster 3	Cluster 1	Cluster 4	Cluster 4	Cluster 4	Cluster 1
		<80%	<80%	80.62%	81.17%	82.17%	82.72%	83.88%	83.73%	83.19%	83.32%
	Best fit							Cluster 1			
				81.54%	82.49%	87.17%	87.50%	91.58%	91.18%	89.73%	89.75%
1 peak	AVG fit				Cluster 1	Cluster 4	Cluster 3	Cluster 1	Cluster 1	Cluster 1	Cluster 2
		<80%	<80%	<80%	<80%	81.14%	81.24%	81.97%	81.93%	82.29%	82.20%
	Best fit					84.65%	84.68%	86.74%	88.65%	88.00%	88.49%
2 peaks	AVG fit					Cluster 1	Cluster 3	Cluster 4	Cluster 3	Cluster 4	Cluster 4
		<80%	<80%	<80%	<80%	80.74%	80.67%	81.74%	81.73%	82.07%	82.24%
	Best fit								Cluster 1		
						82.59%	82.67%	86.18%	85.62%	88.14%	90.11%
3 peaks	AVG fit					Cluster 1	Cluster 2	Cluster 5	Cluster 2	Cluster 2	Cluster 6
		<80%	<80%	<80%	<80%	<80%	<80%	81.63%	81.70%	82.37%	82.21%
	Best fit									Cluster 1	
								84.10%	85.15%	89.58%	88.72%
3+ peaks	AVG fit					Cluster 1		Cluster 2	Cluster 3	Cluster 5	Cluster 6
		<80%	<80%	<80%	<80%	<80%	<80%	81.44%	81.66%	83.36%	82.95%
	Best fit							83.55%	84.09%	88.35%	88.82%